

FABRICATION AND CHARACTERIZATION OF CENTRIFUGAL SPUN CIPROFLOXACIN-LOADED MICROFIBER DRESSING FOR THE TREATMENT OF DIABETIC FOOT ULCERS

Mohd Fareed Shaikh^{a*}, Payaam Vohra^b and Jaya Agnihotri^a

(Received 02 October 2023) (Accepted 29 May 2024)

ABSTRACT

Diabetic Foot Ulcers (DFUs) are open ulcers or sores on the foot with a bony prominence. They are a frequent manifestation of uncontrolled diabetes mellitus and often increase the risk of infection. DFUs typically take longer to heal, sometimes resulting in severe complications such as amputation. Our study aimed to develop a drug delivery system that could help to manage DFUs. We developed polymer-based fibers that were loaded with ciprofloxacin HCl via centrifugal spinning setup. The optimized polymeric fiber batch demonstrated over 90% drug entrapment, controlled drug release for 72 h, an average fiber diameter of 4.88 μm and porosity above 70%. The drug-loaded fibers showed antibacterial action against gram-negative (*E. coli*) and gram-positive (*S. aureus*) pathogens that are often prevalent in DFUs. Additionally, the fibers showed excellent hemocompatibility. Our study's findings show great potential in managing DFUs, and future studies will explore the potential application of this drug delivery system in treating and managing diabetic foot ulcers.

Keywords: Diabetic foot ulcer, diabetic foot infection, ciprofloxacin, polymeric fibers, nanofiber, microfiber centrifugal spinning

INTRODUCTION

Diabetic Foot Ulcers (DFUs) are becoming more common in patients with uncontrolled diabetes mellitus. Lesions or injuries on the lower extremities, particularly the foot, are commonly observed in diabetes mellitus. These wounds have a bony prominence, which creates higher chances of infection. The most visible sign of a foot ulcer is black tissue called eschar. An odorless discharge, partial numbness and inflammatory sensations are associated with DFUs. Foot ulcers pose significant challenges in management and treatment because of their prolonged/delayed healing time, increased risk of infection and potential for severe complications like amputation. Compared with other diabetic complications, DFUs have a higher hospitalization rate, incidence rate and mortality rate, further highlighting the urgent need for effective prevention and treatment strategies. By the end of 2030, diabetes mellitus is projected to be one of the largest global diseases¹. Worldwide, around 18.6 million

cases (2023 figures) are witnessed for people suffering from Diabetic Foot Ulcers. It is roughly estimated that 15-25% of the population with diabetes can develop complications like DFUs. The occurrence of these DFUs is not limited to any age group. However, it is most often seen among individuals 45 or older. The highest incidence of foot ulcers is observed in Latinos, African Americans and Native Americans US²⁻⁵.

A diabetic foot ulcer progresses through three stages: callus formation, motor neuropathy and subcutaneous bleeding.

- 1) The creation of the callus is the initial stage. This callus is developed because of neuropathy.
- 2) Motor neuropathy can induce frequent aberrations^{6,7}. Another factor is autonomic neuropathy, which causes the skin to dry out.
- 3) Repeated injury to the callus leads to subcutaneous bleeding, which eventually erodes into an ulcer⁸⁻¹⁰.

Peripheral neuropathy causes intrinsic muscle atrophy, which results in hammertoe formation and the

^a Department of Pharmaceutics, HK College of Pharmacy, Mumbai- 400 064, Maharashtra, India

^b Department of Pharmacology, NIPER Mohali, SAS Nagar- 160 062, Punjab, India

*For Correspondence: E-mail: far28id1999@gmail.com

<https://doi.org/10.53879/id.61.07.14383>

growth of high-pressure zones at the metatarsal heads on the plantar surface of the foot. A further contributing factor to the occurrence of diabetic foot infections in people with diabetes mellitus is the presence of significant atherosclerosis in the small blood vessels of the lower extremities. This disease leads to impaired vascular function. Necrosis and gangrene are severe complications due to lack of blood reaching the site, leading to delayed wound healing¹¹⁻¹³. DFUs are associated with several etiological factors. Foot deformities, peripheral arteriolar diseases and many more conditions are now common complications for diabetic patients.

The main reason to select ciprofloxacin in our study is because of its broad-spectrum anti-infective activity. It is very well known that infection is one of the significant risk factors related to amputation. Polymicrobial infections commonly occur in diabetic foot ulcers (DFUs), with the involvement of two or more pathogens observed in approximately 75% of cases. The identification of bacterial and fungal pathogens in diabetic foot ulcers (DFUs) can vary depending on factors such as the patient's medical conditions, the location and severity of the ulcer, and previous antibiotic therapy. Commonly found pathogens in diabetic foot ulcers include gram-negative bacteria (*P. aeruginosa*, *K. pneumoniae*, and *E. coli*), gram-positive bacteria (*S. aureus*), and fungi (*C. albicans*)^{14,15}. There are a number of drugs to manage fungal manifestation like azoles, allylamines, etc. Polymers can be employed in treating diabetic wounds because of their outstanding mechanical, bioinert and biodegradable properties^{16,17}.

The rationale for choosing polymeric fibers as a drug delivery system is because of their nature to combat biofilm formation, which is one of the leading causes of antimicrobial resistance. Reducing the biofilm formation can provide a rationalized approach to manage DFU. Polymeric fibers can be formed by using many methods like electrospinning, melt spinning, wet spinning and centrifugal spinning. Centrifugal spinning (force spinning or rotary jet spinning) is a quick and efficient method for producing polymeric nanofibers and microfibers. It utilizes centrifugal force instead of high voltage for stretching and deposition. Centrifugally spun polymeric fiber has been shown to provide optimal attributes for tissue scaffolds. This approach enables the production of microfiber structures with a wide range of desired forms, morphologies and orientations, including beaded, textured or smooth configurations by manipulating the process factors, such as concentration and viscosity. The centrifugal spinning process is preferred over other

methods owing to its comparatively simple mechanism and high production output. The conductivity of the solution does not play a significant role in fiber manufacturing by centrifugal spinning. Therefore, it may be used in a diverse range of polymer emulsions and suspensions, resulting in much greater production rates compared to conventional electrospinning techniques¹⁸⁻²³. The primary objectives of the current research were to develop and characterize a novel polymeric fibers-based drug delivery system for the effective treatment of DFUs and to reduce the number of amputations case due to DFUs. In the current research, our focus was on providing an holistic approach in ciprofloxacin-loaded polymeric fibers to avoid wound infestation by bacteria and prevent wound debridement.

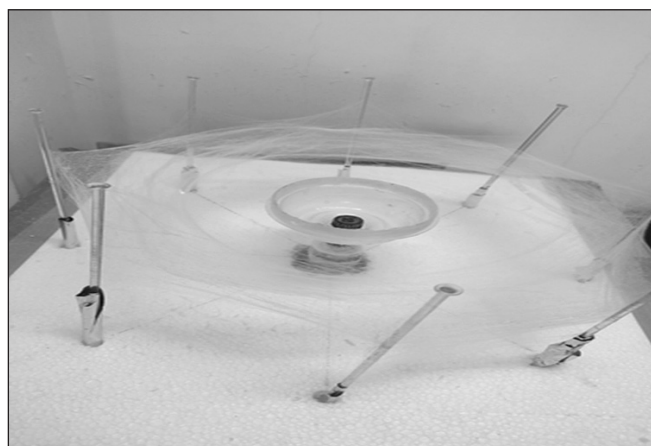


Fig. 1: Centrifugal spinning setup

MATERIALS AND METHODS

Materials

A sample of ciprofloxacin HCl was gifted by Medley Pharmaceuticals Ltd., Mumbai, India, while polyvinyl pyrrolidone K 90 (PVPK90) and ethyl cellulose (EC) were procured from Vishal Chem, Mumbai, India.

Methods

Preparation of feeding polymer solution

In a solvent system (90 parts ethanol and 10 parts water), 1 % w/w drug was added, and then the mixture was stirred using a magnetic stirrer at a speed of 300 rpm until the drug was dissolved. Next, the EC was added and stirred at 500 rpm for 10-15 minutes until completely dissolved. After that, PVPK 90 was added to the solution and stirred at 500 rpm for another 10 minutes (quantities mentioned in Table I). The resulting solution was then carefully stored at room temperature for the fabrication of fiber^{24,25}.

Centrifugal spinning of prepared feeding polymer solution

In the college laboratory, we have developed and optimized the centrifugal spinning system, consisting of a motor shaft for stirring, a polypropylene lid as a spinneret, and a glass rod covered in aluminum foil as a collector (Fig. 1). Gradually, the prepared feeding solution is introduced into this system at a controlled rate of 3 mL min⁻¹, the motor is started, and when the spinneret is spun at a speed of 3000 rpm, within moments, the resultant fibers emerge from the twin nozzles, gathering on the collector surface. In the post-fabrication process, the drug-loaded microfibers are gently air-dried in an enclosed environment at ambient temperature. Once thoroughly dried, these microfibers are cut to precise lengths to meet specific requirements^{26,27}.

Table I: Optimized batches

Batch No	PVPK90 (in parts)	EC (in parts)
F1	97.5	2.5
F2	95	5
F3	90	10

CHARACTERIZATION AND EVALUATION

Entrapment efficiency

The entrapment efficiency of the polymeric microfibers was assessed by subjecting the drug-loaded fibers to a drying process at a temperature of 40°C using a hot air oven. Subsequently, a mat composed of fibers with a predetermined weight was extracted and dissolved in its respective dissolving solvent, which, in this case, was ethanol. The quantity of drug present in the respective solutions was assessed using UV Spectroscopy, and from this data, the amount of drug loaded in fiber was determined. By using equation 1, entrapment efficiency was determined. The experiment was conducted in triplicate^{28,29}.

$$\text{Entrapment efficiency (\%)} = \frac{\text{drug entrapped}}{\text{total drug added}} \times 100$$

....Equation 1

Fiber size and morphology

The analysis of fiber morphology was conducted via a scanning electron microscope. After being coated within a thin layer of gold using a sputter coater, the produced polymeric fibers were scanned using a scanning electron

microscope (EVO 18, Carl Zeiss IIT Roorkee). The average diameter of the polymeric fibers was determined by employing ImageJ V1.48 software. 300 random measurements were conducted at different locations, and the average of the calculated values was determined.

In vitro drug release

The measurement of drug release from polymeric fibers included placing a specific weight of fibers, loaded with the medication, into a 10 mL solution of phosphate buffer saline (PBS). The release investigations were performed at 37°C and at a stirring rate of 100 rpm using a magnetic stirrer. Samples of 1 mL were obtained from the buffer solution at different time intervals, namely at 0.5, 1, 2, 3, 4, 5, 6, 7, 8, 24, 48 and 72 h. After the completion of each sample procedure, the volume was refilled with fresh medium. The drug concentration in the release buffer was determined using a UV-spectrophotometer at 271 nm. Each sample was tested three times, and the average values were recorded. The drug release percentage was determined using the drug's calibration curve in PBS 7.4^{30,31}.

Fourier-transform infrared spectroscopy (FTIR) analysis

The prepared polymeric fibers were characterized using Fourier-transform infrared spectroscopy (FTIR), utilizing KBr pellets to assess the stability and integrity of the drug in polymeric fiber.

pH alteration during scaffold degradation

Polymeric fibers were immersed in a 7.4 buffer solution at 37°C for 60 days. A pH meter was used to measure the pH of the buffer solution^{32, 33}.

Porosity

The measurement of the porosity of the polymeric fiber dressings was conducted using the liquid displacement method. The weight of the mat, denoted as W, was measured by submerging it in a graduated cylinder that contained a specified volume (V₁) of distilled water. The volume that ensued was quantified and documented as V₂. Following 10 minutes, the specimens were withdrawn, and the residual quantity of water was duly recorded (V₃). Subsequently, the determination of the porosity of the polymeric fiber was conducted using equation 2³³.

$$\text{Porosity (\%)} = \frac{(V_1 - V_3)}{(V_2 - V_3)} \times 100$$

....Equation 2

Water vapor permeability (WVP) test

The water vapor permeability (WVP) of the designed dressings was assessed using the bottle permeation test. The dressing bottles were incubated at 33°C for 24 h. The quantification of water evaporated through the dressing was conducted, and Equation 3 was used to determine the water vapor permeability (WVP) of the polymeric fiber. The negative control group comprised of a bottle that did not include any dressing, whereas the positive control group consisted of a bottle that had cotton dressing.

$$WVP = (W/AT) \quad \dots \text{Equation 3}$$

where W, A and T represent the mass of water lost, area (1.327cm²) of dressing, and exposure time, respectively³⁴.

% Water uptake evaluation

The dry polymeric fibre was weighed (W₀) and then placed in distilled water at room temperature. After 30 minutes, the extra water was removed, and the samples were weighed again (W₁). The water absorption ability of the dressings was subsequently determined using Equation 4^{35,36}.

$$\% \text{Water uptake} = \frac{W_1 - W_0}{W_1} \times 100 \quad \dots \text{Equation 4}$$

%Weight loss measurement

The dressings' weight loss was measured to study their degradation. For this, an appropriate quantity of polymeric fiber was measured (W₀), immersed in a PBS solution, removed from the solution after 3, 5 and 7 days, and accurately measured (W₁). Weight loss is determined using Equation 5³⁵.

$$\% \text{Weight loss measurement} = \frac{W_0 - W_1}{W_0} \times 100 \quad \dots \text{Equation 5}$$

Antimicrobial studies test

The disc diffusion method is a widely employed technique for evaluating the antimicrobial efficacy of antibiotics by measuring the zone of inhibition on an agar plate. This method spreads a microbial inoculum (*S. aureus* or *E. coli*) evenly across the agar surface. Next, a polymeric microfibre mat containing the drug is positioned at the center of the plate. The plates are incubated at 32±2.5°C for 24 h. The antimicrobial agent diffuses and exhibits inhibitory effects on microorganisms. The

zone of inhibition size is a significant factor in assessing antimicrobial activity. The diameter of the zone of inhibition was measured^{32,37}.

Hemo - Compatibility test

A drop or two of fresh blood was obtained in a clean tube or container, and then an equivalent volume of formulation was added to the blood sample and gently mixed. This results in a one-to-one dilution of the formulation extract. This combination was incubated for 1 h at 37°C. A little drop of the mixture was put on a glass slide, topped with a coverslip, and gently pushed down to disseminate the sample. Ghost cells were searched. They are the remnants of red blood cells that have lost their interior contents owing to hemolysis. They were viewed under a Digital microscope. Ghost cells have the form of empty, pale, or transparent cells. In this process, distilled water was the positive control, while saline was the negative control^{31,36}.

RESULTS AND DISCUSSIONS

Entrapment efficiency

Table II shows the entrapment efficiency results for F1, F2, and F3 batches, with 91%, 94%, and 86%, respectively. The analysis of the outcomes suggests that the entrapment efficiency of F1 and F2 batches are satisfactory for further investigations. However, the entrapping efficiency of the F3 batch is lower than expected. Therefore, excluding the F3 batch from further investigations is advisable because of its comparatively lower entrapping efficiency. The focus of further characterization will be on F1 and F2 batches, which have shown higher entrapping efficiencies.

Table II: Entrapment efficiency of 3 batches

Batch No.	%EE
F1	91%
F2	94%
F3	86%

Fiber size and morphology

Examining the scanning electron microscope (SEM) pictures (Fig. 2a & 2b) has provided valuable findings on the morphological characteristics of both F1 and F2 batches. Specifically, batch F1 has an average fiber diameter of around 10.41 µm. Interestingly, the variation

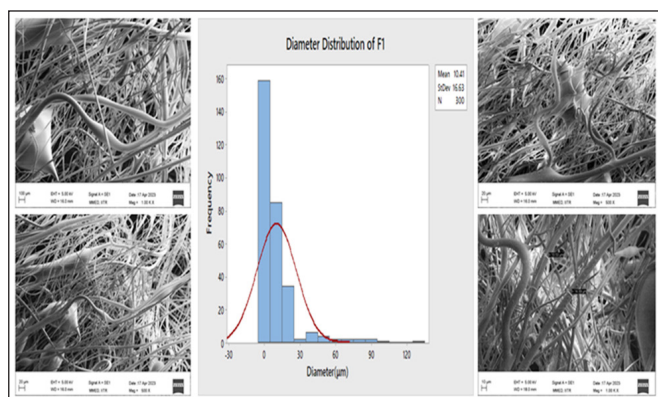


Fig. 2a: SEM images and diameter distribution of F1 batch

of fiber diameters in this batch is broad. Furthermore, the scanning electron microscopy (SEM) photographs of batch F1 demonstrate the existence of beaded fibers within the composition of the batch.

In contrast, the scanning electron microscopy (SEM) imaging of batch F2 presents an opposite situation. The fibers observed in this sample have a notably reduced mean diameter, measuring roughly 4.88 μm. Significantly, the fibers in this particular batch have a uniform and regular surface morphology, characterized by the absence of the bead-like features found in batch F1.

***In vitro* drug release study**

The drug-loaded polymeric fibers from batches F1 and F2 were observed for 72 h to determine their cumulative release (Fig. 3). The data demonstrated a distinct two-stage drug release pattern, consisting of an initial rapid release phase and a subsequent sustained release phase. The release pattern is caused by the initial swelling and then breakdown of the polymeric fiber mats, leading to an initial burst release of the drug followed by gradual

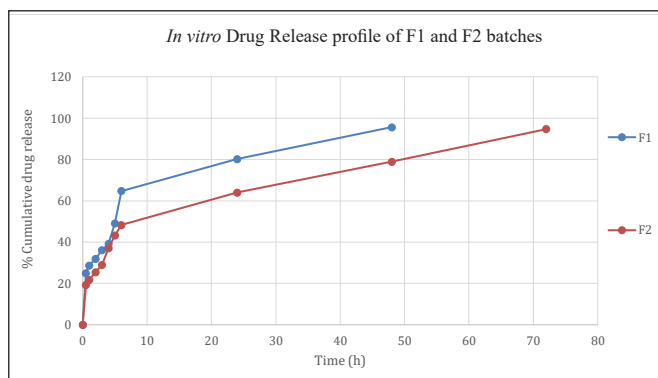


Fig. 3: *In vitro* drug release profile of F1 and F2 batches

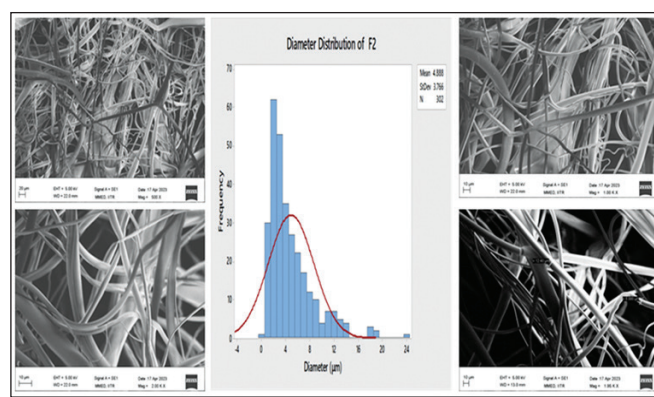


Fig. 2b: SEM images and diameter distribution of F2 batch

dissolution. These mats tend to absorb fluids and degrade, releasing the drug quickly.

Batch F1 exhibits a higher drug release rate, achieving complete drug content release over a span of 48 h. In contrast, batch F2 shows a prolonged initial burst release, which, although slower than F1, has a longer duration. This leads to a sustained release profile that spans the entire 72 h duration. The extended-release pattern is considered more favorable and advantageous in DFU. Based on the results, batch F2 emerges as the optimized batch (Fig. 3). The investigations and characterizations were explicitly centered on this batch F2.

FTIR analysis

It was observed in the FTIR analysis (Fig. 4a & 4b) of the ciprofloxacin polymeric fiber that the key functional groups of ciprofloxacin HCL were still present in polymeric fiber, indicating that the drug is still unchanged in the formulation. The presence of intermolecular hydrogen bonding in the formulation was confirmed by the characteristic peak observed between 3500 and 3450 cm^{-1} , which corresponds to the OH stretching vibration. Furthermore, the FTIR spectra of the fiber exhibit bands at 1700 cm^{-1} , indicating the stretching of carbonyl C = O, and a peak at 1650 cm^{-1} , which is attributed to quinolones. The presence of peaks at 1450 cm^{-1} , corresponding to $\nu\text{C-O}$, and at 1300 to 1250 cm^{-1} , indicating the bending vibration of the O-H group (indicative of carboxylic acid), was observed. Furthermore, the formulation displayed a prominent absorption peak in the range of 1050 to 1000 cm^{-1} , which was attributed to the presence of the C-F functional group. These findings suggest that all vital functional groups peak of ciprofloxacin HCL remain unchanged in the ciprofloxacin-loaded polymeric fiber, indicating the drug's stability and integrity in the polymeric fiber loaded with the drugs.

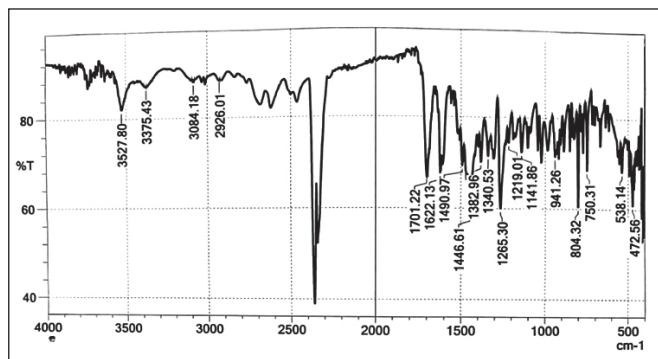


Fig. 4a: FTIR spectra of ciprofloxacin HCl

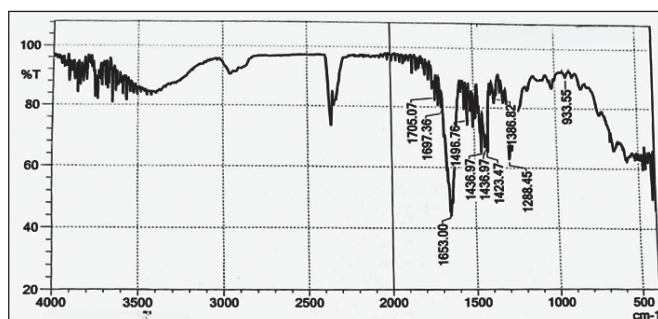


Fig. 4b: FTIR spectra of polymeric fiber batch F2

pH alteration during scaffold degradation

The pH fluctuations of the polymeric fiber solution were observed over 60 days using a phosphate buffer with a pH of 7.4. Fig. 5 effectively demonstrates the graphical depiction of the observations. The results show a noticeable pattern in the trajectory of pH. At the outset, there is a prominent and rapid reduction in pH, signifying a pronounced fall in its numerical magnitude. The observed initial decrease may be attributed to ciprofloxacin

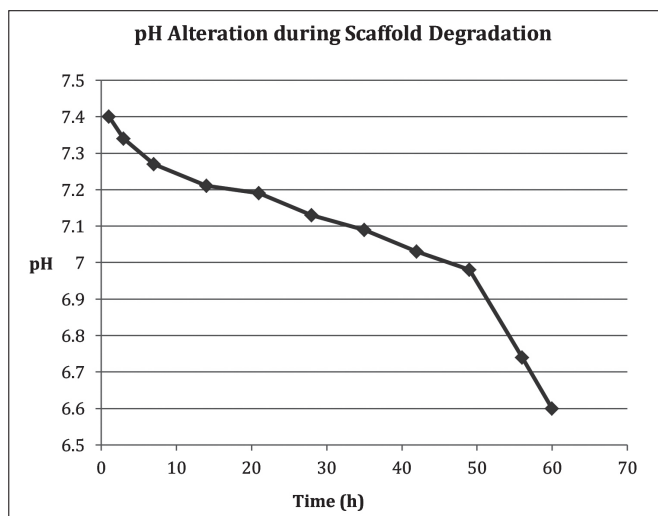


Fig. 5: pH alteration during scaffold degradation profile

hydrochloride salt in the solution, which tends to dissociate, forming both HCl and ciprofloxacin species. Including HCl molecules has a substantial role in the first pH reduction, confirming the observed fast decrease. Nevertheless, an observable alteration in the pH trend becomes evident over time. The pH reaches a condition of equilibrium with negligible fluctuations. The observed phenomenon arises due to the reduced number of available hydrogen chloride (HCl) molecules within the solution. Simultaneously, it is anticipated that the deterioration of constituents such as PVPK90 and EC would cause a transition of the solution toward a neutral state³³.

Porosity

The liquid displacement technique was used to determine the porosity of the produced polymeric fibers. According to the information, the average porosity of the F2 batch was found to be 70.48%. It is important to note that Chong *et al.*³⁴ have suggested porosities ranging from 60% to 90% for tissue engineering purposes. However, even though the porosity of the produced polymeric fibers is within the permitted range, it is crucial to consider other variables. The assessment of Water Vapour Permeability (WVP) is essential to assess the efficacy of the produced polymeric fibers comprehensively.

Water vapour permeability (WVP)

The vapour exchange that occurs through the dressing is a critical attribute that significantly impacts the dressing's overall efficacy. When the WVP value is significantly increased, there is a risk of dehydrating the wound, which promotes the undesired formation of scars. A significantly lower WVP value, on the other hand, may induce a delay in wound healing owing to fluid accumulation on the wound site. As a result, a well-designed dressing should demonstrate an ideal threshold for WVP, striking a careful balance between two opposing results. The WVP test (Fig. 6) found that the F2 batch's WVP value is 12.89 mg cm⁻² h⁻¹, the Control (open) is

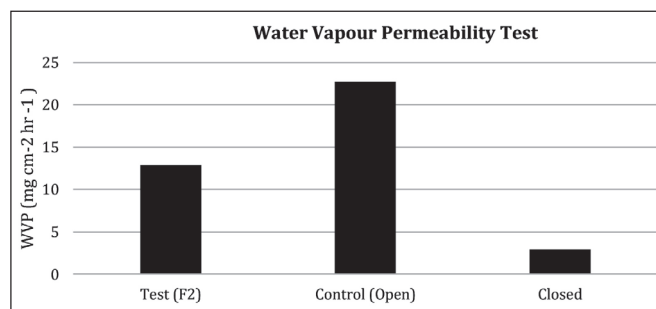


Fig. 6: Water vapor permeability test of batch F2

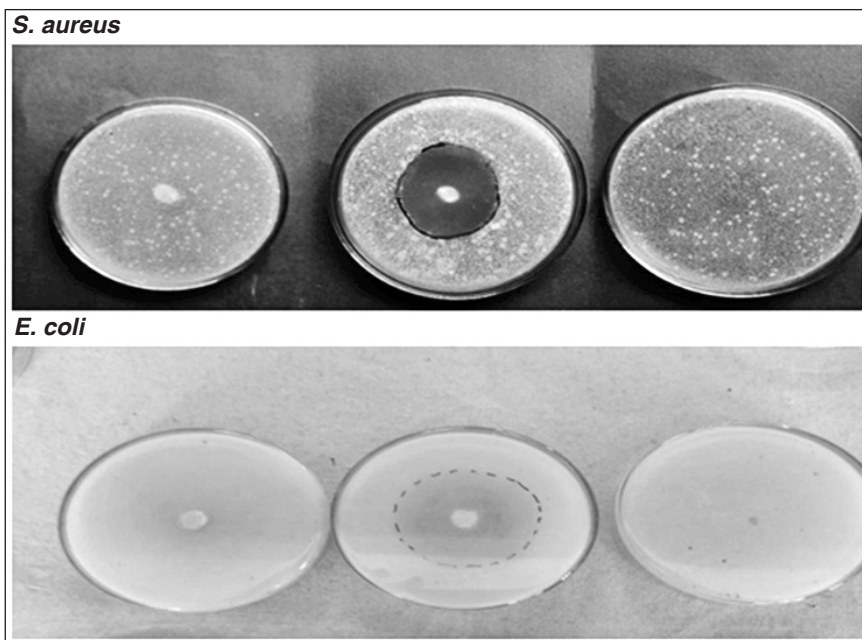


Fig. 7: Antimicrobial activity of ciprofloxacin loaded polymeric fiber on *S. aureus* and *E. coli*

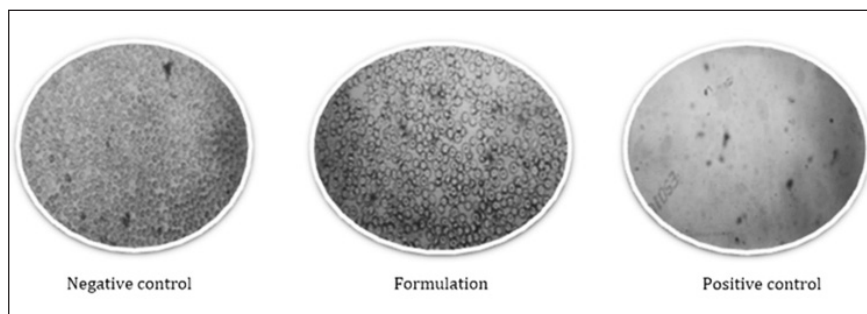


Fig. 8: Hemo-compatibility test

22.73 mg cm⁻² h⁻¹, and the Control (closed) is 2.92 mg cm⁻² h⁻¹. The WVP value of the F2 batch fibers is between open and closed control, which is the desirable value for wound healing.

Water uptake

Water uptake is studied to know whether a dressing can absorb the wound exudate and aid in wound healing. In this study, we found that the optimized batch of F2 polymeric fiber shows a water uptake of 40%. This water absorption is satisfactory, as it is sufficient to manage wound exudate.

Weight loss measurement

The degradation rate of the prepared polymeric fiber was measured in pH 7.4 PBS, and they showed weight loss of 62.71%, 78.57%, and 89.51%, respectively, after 3, 5 and 7 days. The findings revealed that the

developed polymeric fiber dressings lost substantial weight while staying structurally robust, losing 89.51% of their weight after seven days.

Antimicrobial studies test

The test focused on examining the antibacterial characteristics of optimized polymeric fibers batch F2 that was produced; the disc diffusion technique was used to assess antimicrobial activity. Following 48 h, the measurement of the zone of inhibition was conducted. In the *S. aureus* culture, it was observed (Fig. 7) that both the control and blank fiber mat did not exhibit any zone of inhibition. However, a substantial area of inhibition with a diameter of 64 mm was identified in the drug-loaded mat. Similar outcomes have been obtained from the culture of *E. coli*, whereby no noticeable inhibition was seen in the blank and control samples. However, a significant zone of inhibition, approximately 72mm in diameter, was seen on the petri plate with the drug loaded mat. The study results indicate that the polymeric fiber loaded with ciprofloxacin has effective antibacterial properties against the common pathogens *S. aureus* and *E. coli*, often present in wounds associated with DFU.

Hemo-compatibility test

The hemo-compatibility test is a qualitative assessment where a ghost cell is observed in a slide, suggesting an incompatibility between the blood and the formulation due to red blood cell rupture. In this test, we compared the formulation slide and two control groups: the positive control is saline, and the negative control is distilled water. The presence of RBC structures is evident in the positive control and the formulation slide. However, the negative control exhibits many ghost cells, which are nothing but ruptured RBCs (Fig. 8). From the observations, we can conclude that ciprofloxacin polymeric fiber is hemo-compatible.

CONCLUSION

In this research we have effectively fabricated polymer-based fibers loaded with ciprofloxacin, which

exhibits immense potential in managing diabetic foot ulcers. The optimized batch we have obtained has been shown to exhibit remarkable properties, including over 90% drug entrapment, controlled release for 72 h, an average fiber size of 4.88 μm , and porosity above 70%, which is considered adequate for tissue engineering and drug delivery applications. Furthermore, our Fourier-transform infrared spectroscopy (FTIR) investigations have verified the drug's stability and integrity inside the fiber matrix. These results are very encouraging. Furthermore, polymeric fiber has also shown antibacterial effectiveness against *E. coli* and *S. aureus*, which are common pathogens found in diabetic foot infections. In addition, the fiber has displayed excellent hemo-compatibility, thus ensuring compatibility with blood components. We plan to further inspect its potential application in treating diabetic foot ulcers.

REFERENCES

- Lipsky B. A., Aragón-Sánchez J., Diggle M., Embil J., Kono S., Lavery L., Senneville É., Urbančić-Rovan V., Van Asten S., Peters E.J.G., Abbas Z. G., Ertugrul M. B., Jirkovska A., Martinez J. LL., Nather A., Rojas N., Tascini C., Udovichenko O. and Xu Z.: IWGDF guidance on the diagnosis and management of foot infections in persons with diabetes, **Diabetes Metab. Res. Rev.**, 2016, 32, 145-174.
- Deng H., Li B., Shen Q., Zhang C., Kuang L., Chen R., Wang S., Ma Z. and Li G.: Mechanisms of diabetic foot ulceration: A review, **J. Diabetes**, 2023, 15(4), 299-312.
- Armstrong D.G., Boulton A.J.M. and Bus S. A.: Diabetic foot ulcers and their recurrence, **N. Engl. J. Med.**, 2017, 376(24), 2367-2375.
- Mutluoglu M., Uzun G., Turhan V., Gorenek L., Ay H. and Lipsky B.A.: How reliable are cultures of specimens from superficial swabs compared with those of deep tissue in patients with diabetic foot ulcers?, **J. Diabetes Complications**, 2012, 26(3), 225-229.
- Jain S., Kirar, M., Bindeliya, M., Sen L., Soni M., Shan M., Purohit A. and Jain P. K.: Novel drug delivery systems: An overview, **Asian J. Dent. Health Sci.**, 2022, 2(1), 33-39.
- Deng H., Li B., Shen Q., Zhang C., Kuang L., Chen R., Wang S., Ma Z. and Li G.: Mechanisms of diabetic foot ulceration: A review, **J. Diabetes**, 2023, 15(4), 299-312.
- Jhamb S., Vangaveti V.N. and Malabu U.H.: Genetic and molecular basis of diabetic foot ulcers: Clinical review, **J. Tissue Viability**, 2016, 25(4), 229-236.
- Davis F.M., Kimball A., Boniakowski A. and Gallagher K.: Dysfunctional wound healing in diabetic foot ulcers: New crossroads, **Curr. Diabetes Rep.**, 2018, 18(1), 2.
- Yazdanpanah L., Nasiri M. and Adarvishi S.: Literature review on the management of diabetic foot ulcer, **World J. Diabetes**, 2015, 6(1), 37-53.
- Whiting D.R., Guariguata L., Weil C. and Shaw J.: IDF diabetes atlas: Global estimates of the prevalence of Diabetes for 2011 and 2030, **Diabetes Res. Clin. Pract.**, 2011, 94(3), 311-321.
- Snyder R.J. and Hanft J.R.: Diabetic foot ulcers—Effects on QOL, costs, and mortality and the role of standard wound care and advanced-care therapies, **Ostomy Wound Manage**, 2009, 55(11), 28-38.
- Zubair M.A.M.: Diabetic foot ulcer: A review, **Am. J. Intern. Med.**, 2015, 3(2), 28.
- Mirza R.E., Fang M.M., Weinheimer-Haus E.M., Ennis W.J. and Koh T.J.: Sustained inflammasome activity in macrophages impairs wound healing in type 2 diabetic humans and mice, **Diabetes**, 2014, 63(3), 1103-1114.
- Ramirez-Acuña J.M., Cardenas-Cadena S.A., Marquez-Salas P.A., Garza-Veloz I., Perez-Favila A., Cid-Baez M.A., Flores-Morales V. and Martinez-Fierro M.L.: Diabetic foot ulcers: current advances in antimicrobial therapies and emerging treatments, **Antibiotics**, 2019, 8(4), 193.
- Srivastava P. and Sivashanmugam K.: Efficacy of sub-MIC level of meropenem and ciprofloxacin against extensive drug-resistant (XDR) *Pseudomonas aeruginosa* isolates of diabetic foot ulcer patients, **Infect. Genet. Evol.**, 2021, 92.
- Ko A. and Liao C.: Hydrogel wound dressings for diabetic foot ulcer treatment: Status-quo, challenges, and future perspectives, **BME Mat.**, 2023, 1(3), e12037.
- Liu Y., Zhou S., Gao Y. and Zhai Y.: Electrospun nanofibers as a wound dressing for treating diabetic foot ulcer, **Asian J. Pharm. Sci.**, 2019, 14(2), 130-143.
- Sethuram L. and Thomas J.: Therapeutic applications of electrospun nanofibers impregnated with various biological macromolecules for effective wound healing strategy—a review, **Biomed. Pharmacother.**, 2023, 157, 113996.
- IWGDF Guidelines, Available at <https://iwgdfguidelines.org/> (Accessed 29 September 2023).
- Shaheen M.M.A., Al Dahab S., Abu Fada M. and Idieis R.: Isolation and characterization of bacteria from diabetic foot ulcer: Amputation, antibiotic resistance and mortality rate, **Int. J. Diabetes Dev. Countries**, 2022, 42(3), 529-537.
- Jia Z., Gong J., Zeng Y., Ran J., Liu J., Wang K., Xie C., Lu X. and Wang J.: Bioinspired conductive silk microfiber integrated bioelectronic for diagnosis and wound healing in diabetes, **Adv. Funct. Mater.**, 2021, 31(19), 2010461.
- Liu Y., Li C., Feng Z., Han B., Yu D.G. and Wang K.: Advances in the preparation of nanofiber dressings by electrospinning for promoting diabetic wound healing, **Biomolecules**, 2022, 12(12), 1727.
- Noroozi S., Hassanzadeh H., Arne W., Larson R.G. and Taghavi S.M.: Centrifugal spinning of polymeric solutions: Experiments and modelling, **J. Non-Newtonian Fluid Mech.**, 2023, 313, 104971.
- Merchiers J., Meurs W., Deferme W., Peeters R., Buntinx M. and Reddy N.K.: Influence of polymer concentration and nozzle material on centrifugal fiber spinning, **Polymers**, 2020, 12(3), 575.
- Weitz R.T., Harnau L., Rauschenbach S., Burghard M. and Kern K.: Polymer nanofibers via nozzle-free centrifugal spinning, **Nano Lett.**, 2008, 8(4), 1187-1191.
- Hou T., Li X., Lu Y. and Yang B.: Highly porous fibers prepared by centrifugal spinning, **Mater. Des.**, 2017, 114, 303-311.
- Zhang Z.M., Duan Y.S., Xu Q. and Zhang B.: A review on nanofiber fabrication with the effect of high-speed centrifugal force field, **J. Eng. Fibers Fabr.**, 2019, 14.
- Reddy S.G. and Thakur A.: Drug entrapment efficiency of silver nanocomposite hydrogel, **IOP Conf. Ser. Mater. Sci. Eng.**, 2019, 577(1), 012176.
- Kataria K., Gupta A., Rath G., Mathur R.B. and Dhakate S.R.: *In vivo* wound healing performance of drug loaded electrospun composite nanofibers transdermal patch, **Int. J. Pharm.**, 2014, 469(1), 102-110.

30. Moydeen A.M., Ali Padusha M.S., Aboelfetoh E.F., Al-Deyab S.S. and El-Newehy M.H.: Fabrication of electrospun poly(vinyl alcohol)/dextran nanofibers via emulsion process as drug delivery system: Kinetics and *in vitro* release study, **Int. J. Biol. Macromol.**, 2018, 116, 1250-1259.
31. Salimi E., Ghaee A., Ismail A.F., Othman M.H.D. and Sean G.P.: Current approaches in improving hemocompatibility of polymeric membranes for biomedical application, **Macromol. Mater. Eng.**, 2016, 301(7), 771-800.
32. Balouiri M., Sadiki M. and Ibensouda S.K.: Methods for *in vitro* evaluating antimicrobial activity: A review, **J. Pharm. Anal.**, 2016, 6(2), 71-79.
33. Salehi M., Naseri Nosar M., Amani A., Azami M., Tavakol S. and Ghanbari H.: Preparation of pure PLLA, pure chitosan, and PLLA/chitosan blend porous tissue engineering scaffolds by thermally induced phase separation method and evaluation of the corresponding mechanical and biological properties, **Int. J. Polym. Mater. Polym. Biomater.**, 2015, 64(13), 675-682.
34. Chong E.J., Phan T.T., Lim I.J., Zhang Y.Z., Bay B.H., Ramakrishna S. and Lim C.T.: Evaluation of electrospun PCL/gelatin nanofibrous scaffold for wound healing and layered dermal reconstitution, **Acta Biomater.**, 2007, 3(3), 321-330.
35. Samadian H., Zamiri S., Ehterami A., Farzamfar S., Vaez A., Khastar H., Alam M., Ai A., Derakhshankhah H., Allahyari Z., Goodarzi A. and Salehi M.: Electrospun cellulose acetate/gelatin nanofibrous wound dressing containing berberine for diabetic foot ulcer healing: *In vitro* and *in vivo* studies, **Sci. Rep.**, 2020, 10(1), 8312.
36. Farzamfar S., Naseri-Nosar M., Samadian H., Mahakizadeh S., Tajerian R., Rahmati M., Vaez A. and Salehi M.: Taurine-loaded poly(ϵ -caprolactone)/gelatin electrospun mat as a potential wound dressing material: *In vitro* and *in vivo* evaluation, **J. Bioact. Compat. Polym.**, 2018, 33(3), 282-294.
37. Hudzicki J.: Kirby-Bauer disk diffusion susceptibility test protocol, **Am. Soc. Microbiol.**, 2009, 15, 55-63.



NOW AVAILABLE ! IDMA-APA GUIDELINES / TECHNICAL MONOGRAPHS

TECHNICAL MONOGRAPH NO. 1
**STABILITY TESTING OF EXISTING
DRUGS SUBSTANCES AND PRODUCTS**

TECHNICAL MONOGRAPH NO. 3
**INVESTIGATION OF OUT OF SPECIFICATION
(OOS) TEST RESULTS**

TECHNICAL MONOGRAPH NO. 5
**ENVIRONMENTAL MONITORING
IN CLEANROOMS**

TECHNICAL MONOGRAPH NO. 7
DATA INTEGRITY GOVERNANCE

TECHNICAL MONOGRAPH NO. 2
**PRIMARY & SECONDARY CHEMICAL
REFERENCE SUBSTANCES**

TECHNICAL MONOGRAPH NO. 4
**PHARMACEUTICAL PREFORMULATION
ANALYTICAL STUDIES**

TECHNICAL MONOGRAPH NO. 6
**CORRECTIVE/PREVENTIVE ACTIONS
(CAPA) GUIDELINE**

TECHNICAL DOCUMENT NO. 8
**QUALITY 4.0 DIGITAL
TECHNOLOGY OF THE FUTURE**

Copies are available at IDMA Office, Mumbai. We do not mail any publications against VPP payment.
All payments to be made in advance as Cheque/DD/RTGS/NEFT in favour of
"INDIAN DRUG MANUFACTURERS' ASSOCIATION" at Mumbai.

For more details please contact: **PUBLICATIONS DEPARTMENT** Tel.: 022-49729227 / 66626901
E-mail: melvin@idmaindia.com/anjum@idmaindia.com/geeta@idmaindia.com
Website: www.idma-assn.org/www.indiandrugsonline.org